CHEMISTRY
A European Journal

Supporting Information

Pancake Bonding in π-Stacked Trimers in a Salt of Tetrachloroquinone Anion

Krešimir Molčanov,*[a] Zhongyu Mou,[b] Miklos Kertesz,*[b] Biserka Kojić-Prodić,[a] Dietmar Stalke,[c] Serhiy Demeshko,[c] Ana Šantić,[a] and Vladimir Stilinović[d]

chem_201800672_sm_miscellaneous_information.pdf

Two-electron / multicentre - pancake bonding in π-stacked trimers in a salt of tetrachloroquinone anion

Krešimir Molčanov*[a], Zhongyu Mou[b], Miklos Kertesz[b], Biserka Kojić-Prodić[a], Dietmar Stalke[c], Serhiy Demeshko[c], Ana Šantić[a], Vladimir Stilinović[d]

[a] Rudjer Bošković Institute, Bijenička 54, HR-10000 Zagreb, Croatia E-mail: kmolcano@irb.hr
[b] Department of Chemistry and Institute of Soft Matter, Georgetown University, 424 Regents Hall, Washington DC 20057-1227, USA
E-mail: Miklos.Kertesz@georgetown.edu
[c] Institut für Anorgansiche Chemie, Universität Göttingen, Tammanstraβe 4, D-37077 Göttingen, Germany
[d] Department of Chemistry, Faculty of Science, University of Zagreb, Horvatovac 102a, HR-10000 Zagreb, Croatia

Abstract: The crystal structure of [4-damp])$_2$[Cl_4Q]$_3$ (4-damp = 4-dimethylamino-*N*-methylpyridinium, Cl_4Q = tetrachloroquinone) salt is built up from slipped columnar stacks of quinoid rings composed of closely bound trimers with the intra-trimer separation distance of 2.84 Å and total charge of -2 whereas the inter-trimer distance is 3.59 Å. The inidividual rings exhibit partial negative charges that are distributed unevenly among the three Cl_4Qs in the trimer. The strong interactions within a trimer $(Cl_4Q)_3^{2-}$ have a partially covalent character with two-electrons / multi-centered bonding, that is extended over three rings, plausibly termed as 'pancake bonding'. The electron pairing within this multicentre bond leads to the fact that the crystals are diamagnetic and act as insulators. The studies of the structure and nature of bonding are based on X-ray charge density analysis and density functional theory.

DOI: 10.1002/anie.2016XXXXX

Table of Contents

Experimental Procedures

Preparation and crystallization
All reagents and solutions used were purchased from commercial sources (Merck, Sigma Aldrich, Kemika), were of p.a. grade and were used without further purification.
4-dimethylamino-*N*-methylpyridinium iodide was prepared by slowly adding a solution of methyl iodide in acetone (20 mmol in 10 mL) to an acetone solution of 4-dimethylaminopyridine (20 mmol in 10 mL) with stirring. Colorless crystalline solid stared to appear after *ca.* 30 min. After mixing of the reagents, the solution was left to cool to 0 °C, after which 4-dimethylamino-*N*-methylpyridinium iodide was filtered and washed with cold acetone. The title compound was prepared by adding excess of solid 4-dimethylamino-*N*-methylpyridinium iodide into a saturated solution of tetrachloroquinone in cold acetone (20 mL, at 5 °C) after a previously described method [1]. Diffraction-quality single crystals were grown in 3 *h*; acetone solution was then decanted and the crystals were dried. Main Text Paragraph.

Magnetic measurements
Temperature-dependent magnetic susceptibility measurements were carried out with a Quantum-Design MPMS-XL-5 SQUID magnetometer equipped with a 5 T magnet in the range from 295 K to 2 K. The crystalline sample was contained in a Teflon bucket and fixed in a nonmagnetic sample holder. Each raw data file for the magnetic moment was corrected for the diamagnetic contribution of the sample holder and the Teflon bucket. The molar susceptibility data was corrected for the diamagnetic contribution. Simulation of the experimental data with full-matrix diagonalization of exchange coupling and Zeeman splitting was performed with the *julX* program [2].

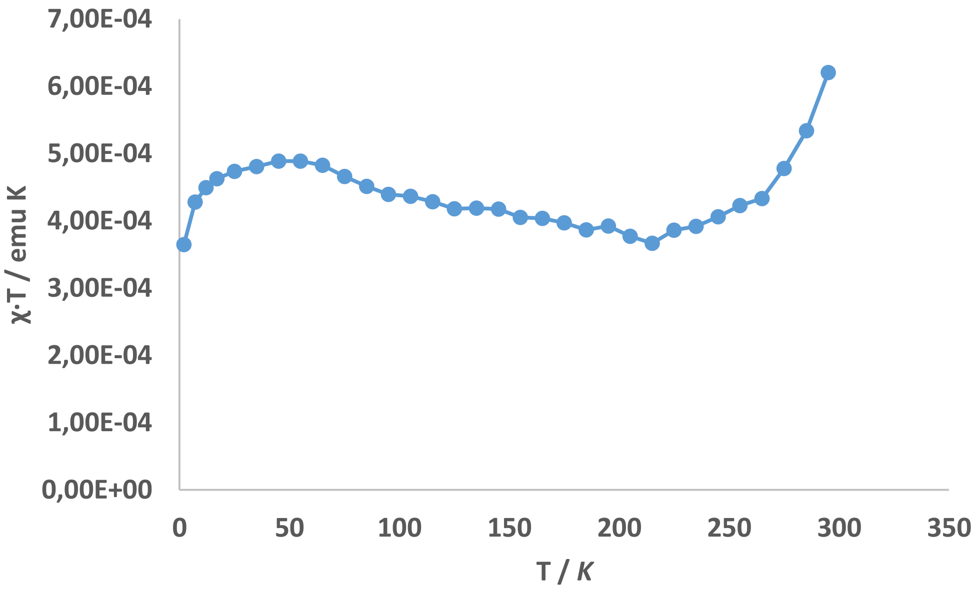

Figure S1. Temperature dependence of magnetization for the title compound.

Electrical measurements

The electrical conductivity of the single crystal in two orientations, [010] (along the direction of stacking) and [100] (normal to the stacks) was measured by impedance spectroscopy (Novocontrol Alpha-N dielectric analyser) in the frequency range 0.01 Hz – 1 MHz at 20 °C. For electrical contact, silver paint electrodes were applied on the opposite surfaces of the crystal [i.e. (100) and ($\bar{1}$00) for one direction and (010) and (0$\bar{1}$0) for the other). The impedance spectra was analysed by equivalent circuit modelling using the complex nonlinear least-squares fitting procedure (ZView software). The complex impedance plane in both crystal orientations displays an arc which can be modelled by an equivalent circuit consisting of a resistor and a capacitor in parallel. The parameters of the equivalent circuit [electrical resistance (R) and capacitance (C)] obtained from the fitting are shown in Figure S2. From the values of electrical resistance (R) and crystal dimensions, DC conductivities were calculated. The electrical conductivity of the single crystal along both directions at 20 °C equals to ≈6.4 x 10^{-13} (Ω cm)$^{-1}$.

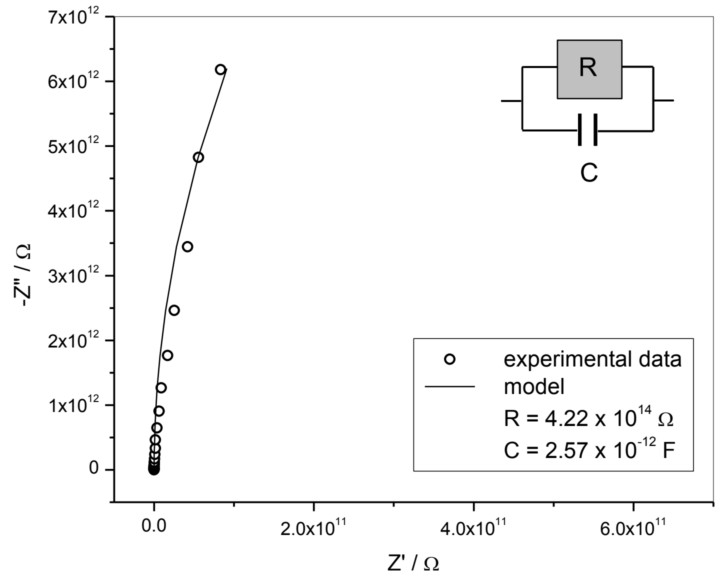

Figure S2. Complex impedance plane of the crystal (measured in the direction [010]) and the corresponding equivalent circuit.

X-ray diffraction and multipolar refinement

Single crystal X-ray diffraction data was collected using a Rigaku Oxford Diffraction XtaLAB Synergy-S diffractometer equipped with a PhotonJET microfocus molybdenum source and a PILATUS3 R 200K-A photon counting detector. The crystal was kept at 100.01(10) K during data collection. Mo*Kα* radiation (λ = 0.71073 Å) was used and the data collection strategy involved several ω scans to achieve a completeness of over 99 % to a resolution of 0.48 Å. 6632 frames were recorded over 76 hours. A total of 182639 reflections were measured, of which 18072 were unique (completeness of 99.9 %, average redundancy of 10.1, R_{int} = 0.042, R_σ = 0.022, average $<F^2/\sigma(F^2)>$ = 33.4).

The software program CrysAlis^Pro (Version 1.171.39) [3] was used for data collection and processing. After integration and scaling, absorption correction methods were applied which included applying a numerical absorption correction based on gaussian integration over a multifaceted crystal model as well as empirical absorption correction using spherical harmonics as implemented in SCALE3 ABSPACK scaling algorithm. Using Olex2, [4] the structure was solved with the ShelXT [5] structure solution program using Intrinsic Phasing and refined with the ShelXL [5] refinement package using Least Squares minimisation.

Multipolar refinement was carried out with program package MoPro [6] *vs*. all reflections F^2*2 up to s = 0.95 Å^{-1}; in the later stages of refinement, reflections beyond this resolution were omitted due to Y_{obs}/Y_{calc} improper scaling. The lengths of the C-H bonds in the cation were constrained to 1.083 and 1.077 Å for methyl and aromatic protons, respectively. Hydrogen atoms were refined as anisotropic, with their $U_{iso's}$ constrained to values derived from quantum chemical calculations; the vibrational modes were estimated by the SHADE3 server. [7] Vibrations of chlorine atoms were refined as anharmonic using third-order Gram-Charlier coefficients.

Geometry and charge-density calculations were performed by MoPro; [6] molecular graphic were prepared using MoProViewer [8] and ORTEP-3. [9] Crystallographic and refinement data are shown in Table S1. Topological bond orders were calculated using the fitted formula [10]

$$n_{topo} = a + b\,\lambda_3 + c\,(\lambda_1 + \lambda_2) + d\,\rho_{cp}\,.$$

SUPPORTING INFORMATION

Coefficients *a*, *b*, *c* and *d* were taken from the literature: for C-C bonds *a* = -0.522, *b* = -1.695, *c* = 0.00, *d* = 8.473; [14] for C-O bonds *a* = -0.427, *b* = -0.240, *c* = 0.280, *d* = 6,464; [12] for C-N bonds *a* = -0.284, *b* = 0.331, *c* = 0.559, *d* = 6.569; [11] for C-H bonds *a* = -0.153, *b* = -0.481, *c* = 0.983, *d* = 8.087. [13]

Table S1. *Crystallographic, data collection and charge-density refinement details*.

Compound	**1**
Empirical formula	$C_{17}H_{13}Cl_6N_2O_3$
Formula wt. / g mol^{-1}	505.99
Crystal dimensions / mm	0.181 x 0.074 x 0.059
Space group	$P\bar{1}$
a / Å	9.7152(1)
b / Å	10.2504(2)
c / Å	11.9006(2)
α / °	115.207(1)
β / °	94.618(1)
γ / °	111.666(1)
Z	2
V / Å^3	955.85(3)
D_{calc} / g cm^{-3}	1.759
μ / mm^{-1}	0.922
Θ range / °	2.35 – 48.28
T / K	100.01(10)
Radiation wavelength	0.71073 (MoKα)
Diffractometer type	XtaLAB Synergy-S
Range of h, k, l	–20 < h < 20; –21 < k < 21; –24 < l < 24
Reflections collected	183679
Independent reflections	26230
reflections with I ≥ 2σ	21336
Absorption correction	Gaussian
T_{min}, T_{max}	0.552, 1.000
Weighting scheme	$w = 1/[1.9641\sigma^2(F_o^2)]$
R_{int}	0.0417
R (F)	0.0312
R_w (F^2)	0.0647
Goodness of fit	1.010
H atom treatment	constrained, anisotropic parameters constrained to calculated values
No. of parameters	961
No. of restraints	454

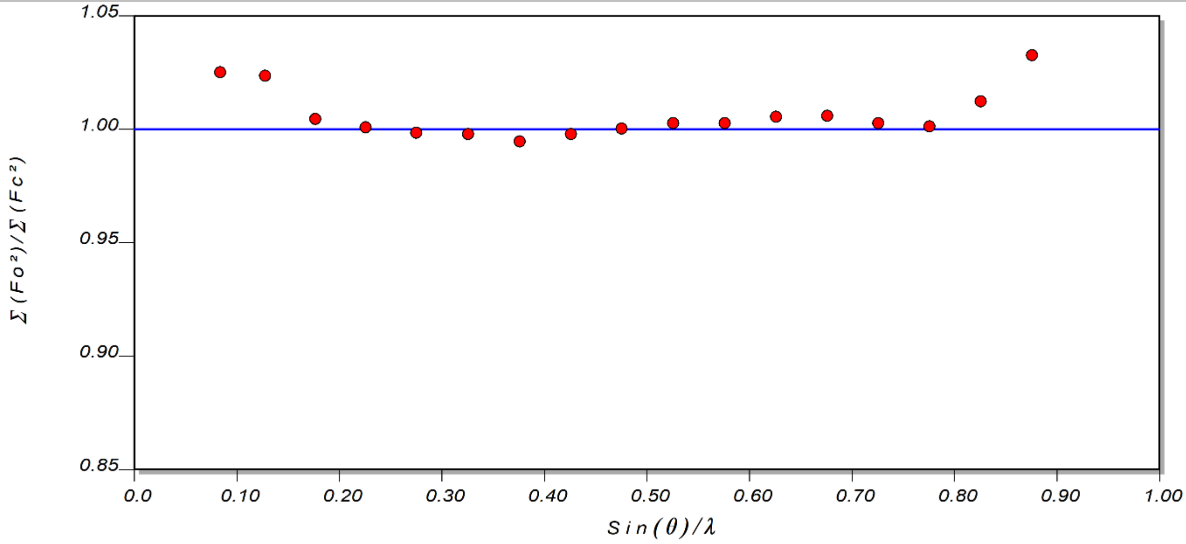

Figure S3. XDRK plot showing the fit of <Y_{obs}> *vs* <Y_{calc}> as a function of resolution.

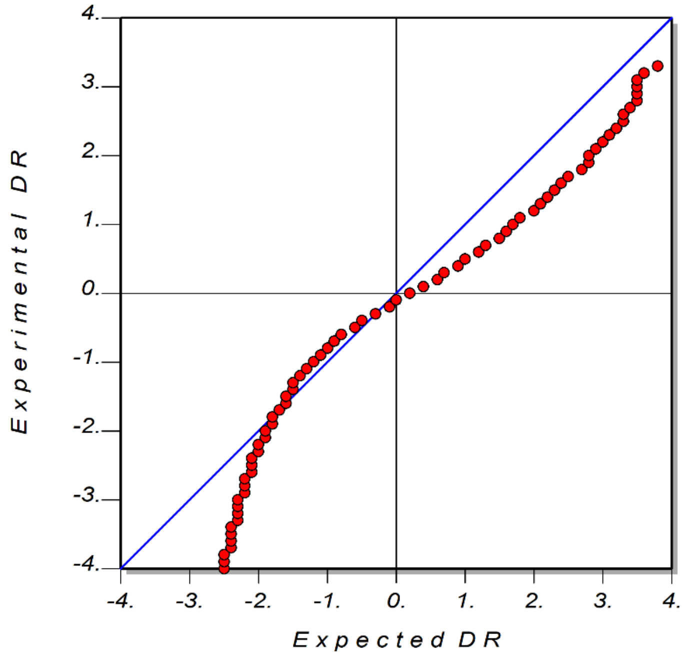

Figure S4. XDRK plot showing the expected and experimental Y_{obs}- Y_{calc} data profile.

Results and Discussion

Details on crystal structure

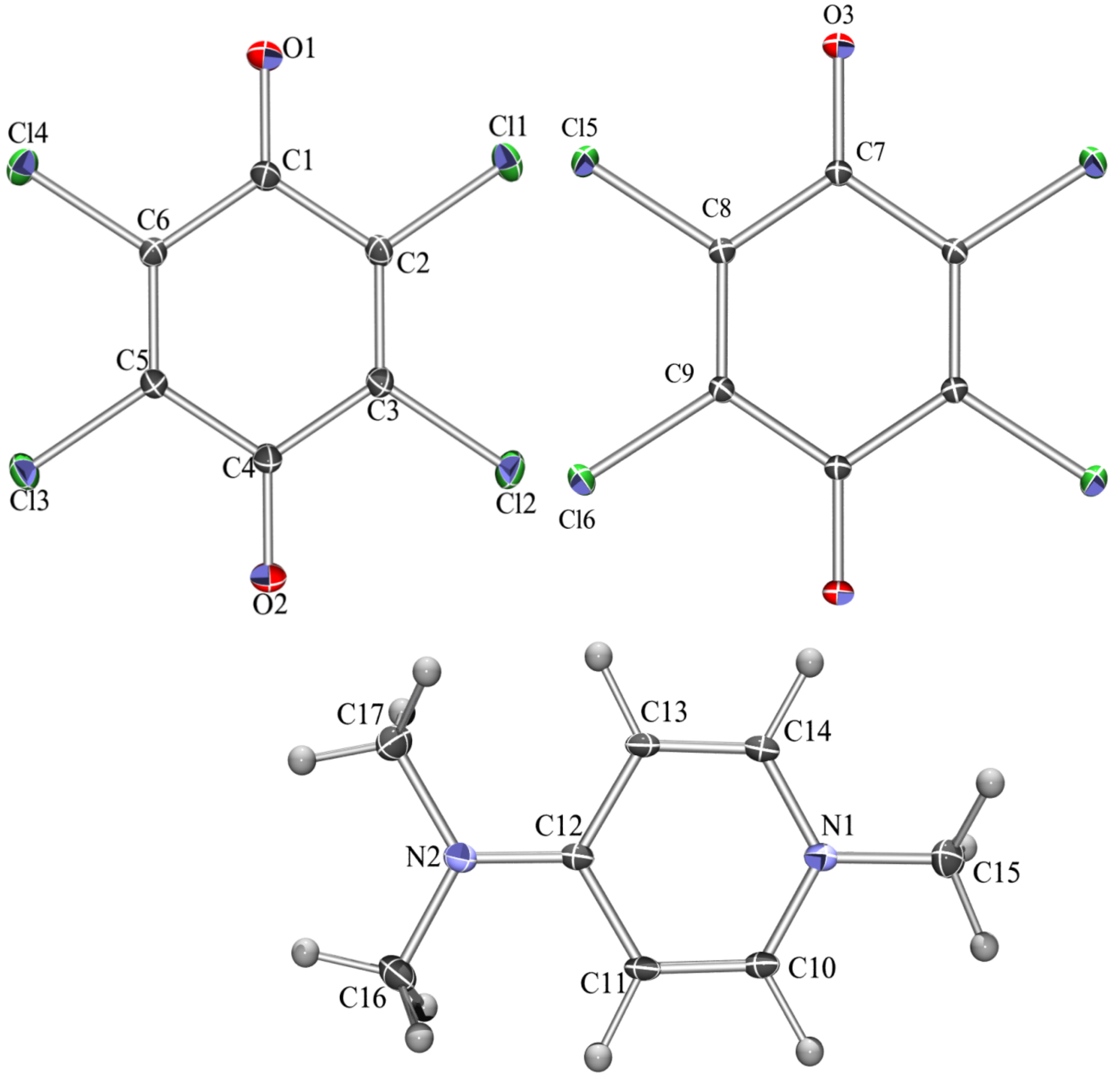

Figure S5. ORTEP drawings of two symmetry-independent quinone anions and the cation. Displacement ellipsoids were drawn to the probability of 50 % and hydrogen atoms are shown as spheres of arbitrary radii.

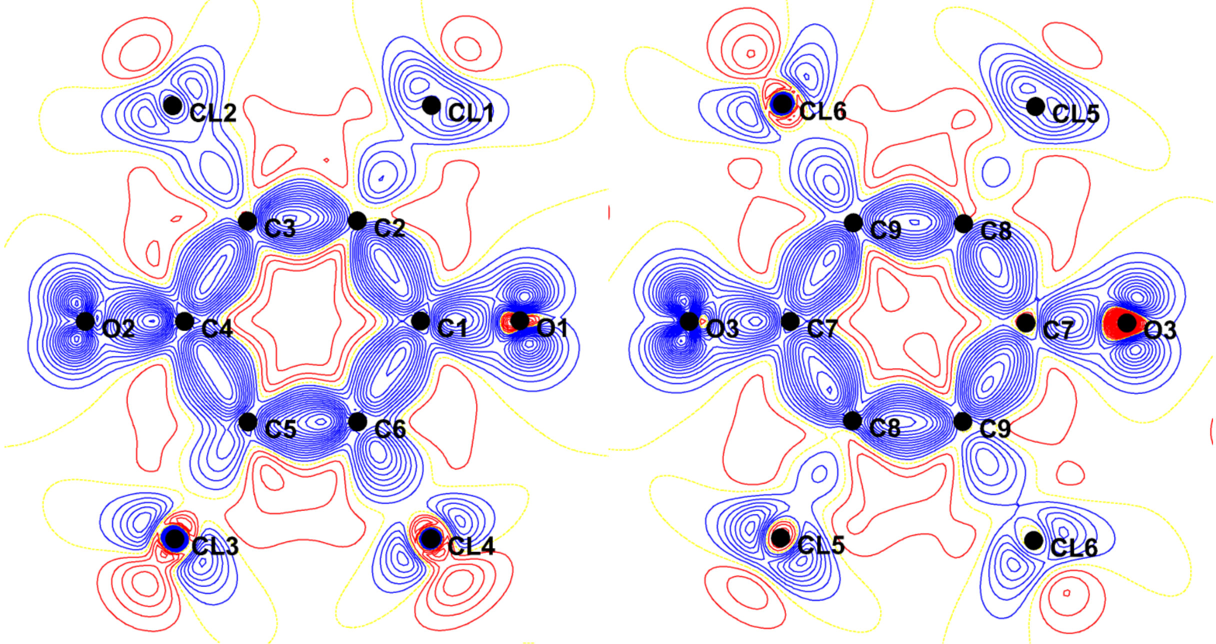

Figure S6. Deformation densities of two symmetry-independent quinoid anions. Positive density is shown in blue and negative in red; yellow dotted lines represent zero density. Contours are drawn for 0.05 eÅ^{-1}. Computed from XRD based densities.

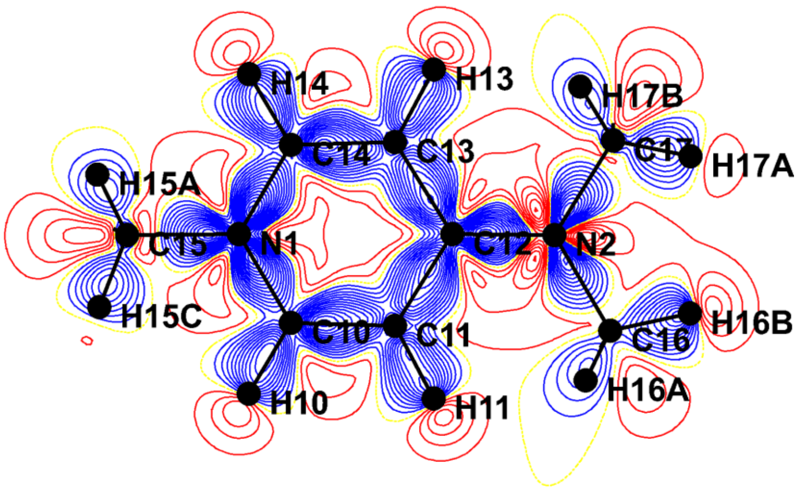

Figure S7. Deformation density of the *N*-methyl-4-dimethylaminopyridinium cation. Positive density is shown in blue and negative in red; yellow dotted lines represent zero density. Contours are drawn for 0.05 eÅ^{-1}. Computed from XRD based densities.

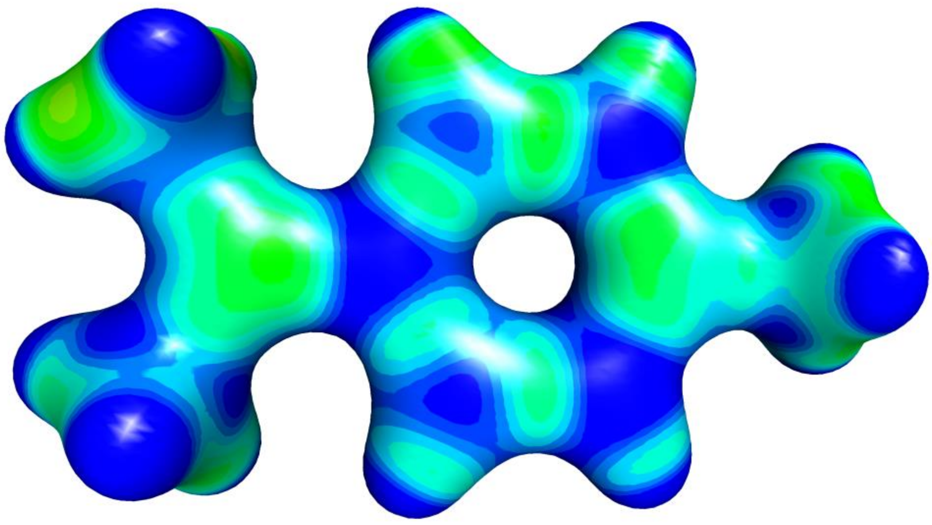

Figure S8. Electrostatic potential derived from X-ray charge density in of the *N*-methyl-4-dimethylaminopyridinium cation plotted onto an electron density isosurface of 0.5 e Å^{-3}. Potential varies from -0.1 (dark red) to +0.8 (dark blue).

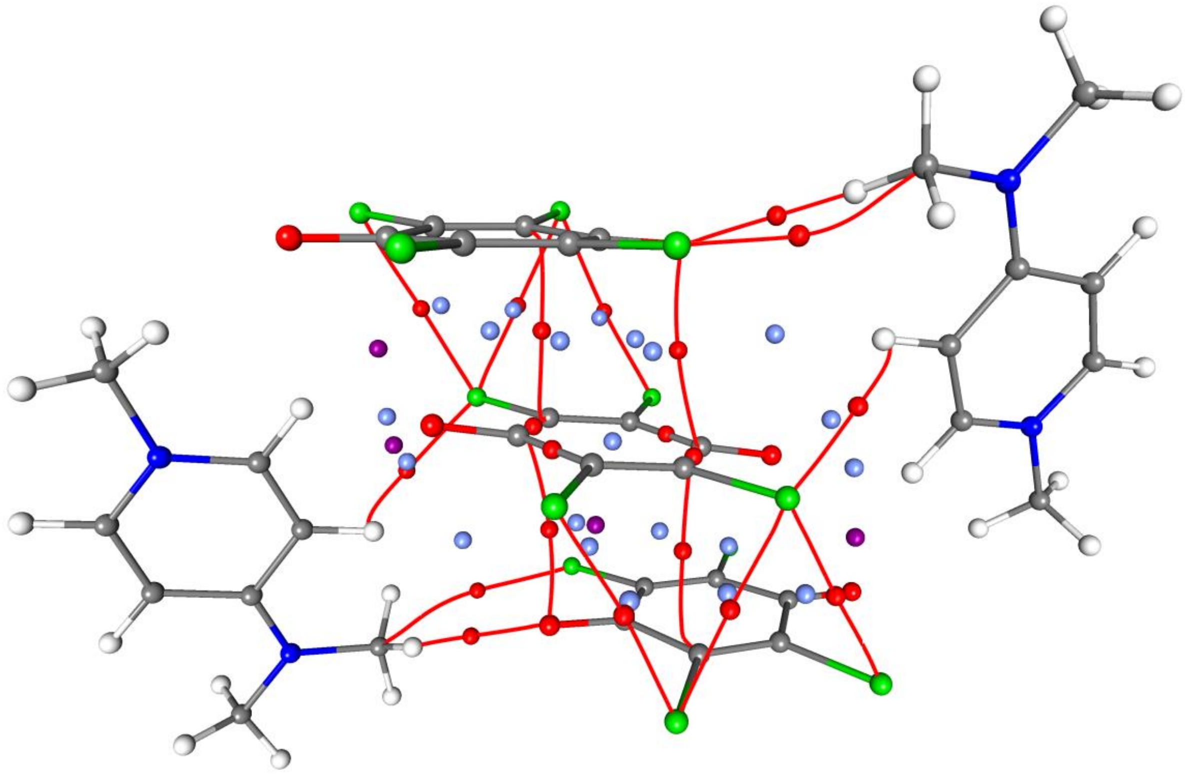

Figure S9. Critical points in **1**. (3,-1) critical points are drawn as red spheres, (3,+1) as light blue and (3,+3) as purple; bond paths are shown as red lines. Computed from XRD based densities.

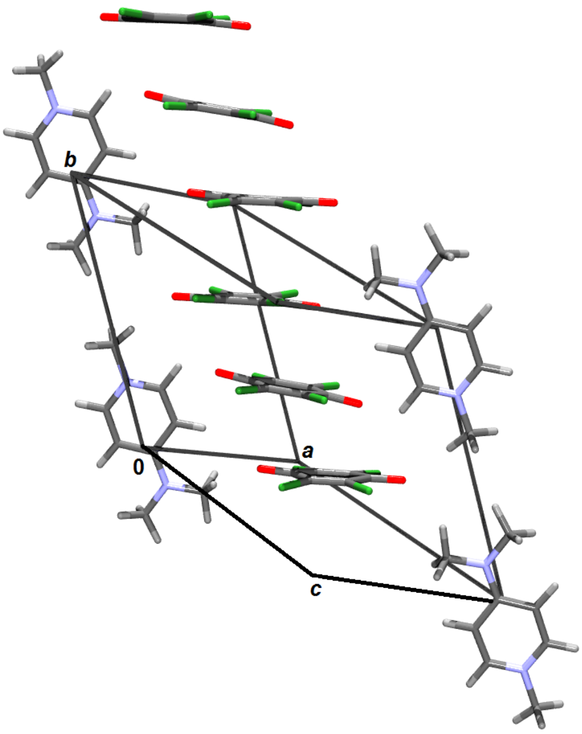

Figure S10. A detail of crystal packing of **1** showing two stacked triplets of quinoid rings. Short intra-triplet contact (pancake bond) is marked as A and the long, inter-triplet contact is marked as B.

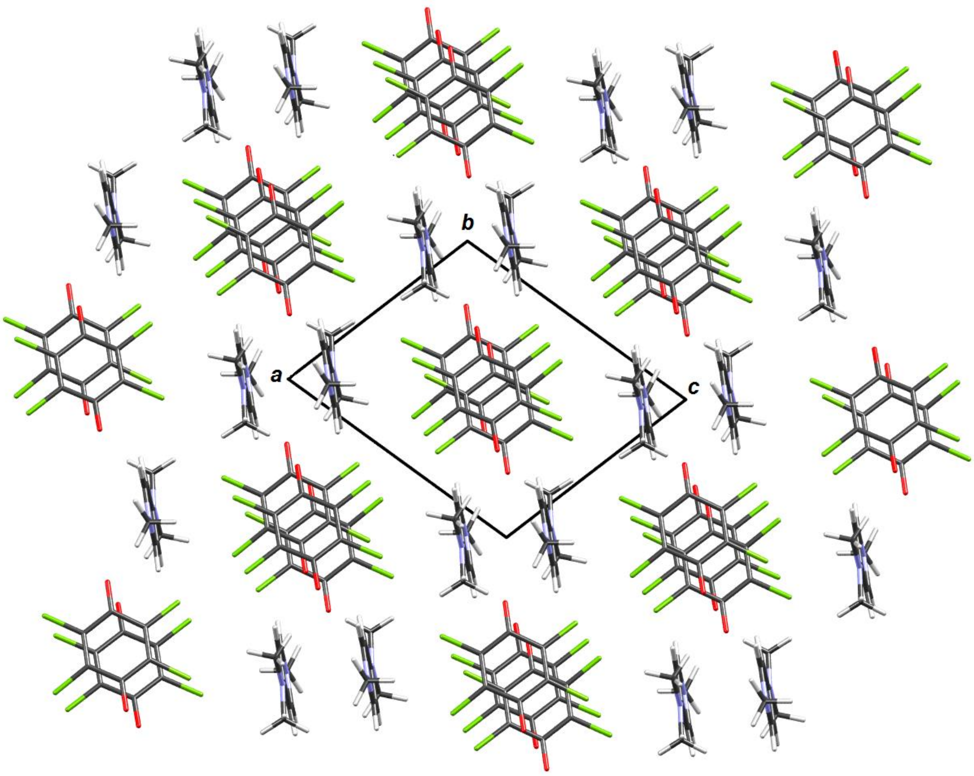

Figure S11. Crystal packing of **1** viewed in the direction [010].

Table S2 Atomic charges (e) in the quinoid moieties derived from P_{val}: $Q = N_{val} - P_{val}$ difference between number of valence electrons in neutral and refined multipolar atom. Esd's were obtained after refinement vs. all variables. Values for neutral Cl_4Q and semiquinone radical [14] are given for comparison. Computed from XRD based densities.

Atom	Quinone **1**		Quinone **2**		Neutral Cl_4Q [14]		Radical [14]
O1	-0.248	O3	-0.253	O1	-0.159	O1	-0.123
Cl1	-0.023	Cl5	-0.006	Cl1	-0.020	Cl1	-0.170
Cl2	-0.038	Cl6	-0.022	Cl2	-0.027	Cl2	-0.173
C1	+0.032	C7	+0.031	C1	+0.305	C1	-0.154
C2	-0.022	C8	-0.108	C2	-0.131	C2	+0.048
C3	+0.024	C9	-0.023	C3	-0.061	C3	+0.048
O2	-0.177					O2	-0.147
Cl3	-0.118					Cl3	-0.171
Cl4	+0.075					Cl4	-0.172
C4	-0.058					C4	-0.100
C5	+0.083					C5	+0.119
C6	-0.117					C6	+0.070
Total charge	-0.587		-0.762		0		-0.925

Table S3. Atomic charges (e) in the *N*-methyl-4-dimethylaminopyridinium cation derived from P_{val}: $Q = N_{val} - P_{val}$ difference between number of valence electrons in neutral and refined multipolar atom. Computed from XRD based densities. Esd's were obtained after refinement vs. all variables.

Atom	P_{val}
N1	-0.072
N2	+0.105
C10	-0.021
C11	+0.073
C12	-0.169
C13	+0.075
C14	-0.022
C15	-0.341
C16	-0.210
C17	-0.341
H10	+0.089
H11	+0.089
H13	+0.091
H14	+0.089
H15A	+0.220
H15B	+0.173
H15C	+0.208
H16A	+0.123
H16B	+0.117
H16C	+0.137
H17A	+0.228
H17B	+0.113
H17C	+0.218
Total charge	+0,972

Table S4. Bond lengths (Å) and Cremer-Pople puckering parameters (τ) [15] of quinoid rings. Lengths of corresponding bonds in neutral Cl_4Q and tetrachlorosemiquinone radical anion from our recent X-ray charge density study [14] are given for comparison. Symmetry operator *i*) 1–*x*, 1–*y*, 1–*z*.

Quinone 1		**Quinone 2**		**Cl_4Q**		**Cl_4Q^- radical anion**	
C1-C2	1.4762(1)	C7-C8	1.4555(1)	C1-C2	1.4901(6)	C1-C2	1.4564(4)
C2-C3	1.3624(1)	C8-C9	1.3724(1)	C2-C3	1.3467(5)	C2-C3	1.3702(3)
C3-C4	1.4740(1)	C9-C7^i	1.4548(1)	C1-C3^i	1.4897(6)	C3-C4	1.4563(4)
C4-C5	1.4752(1)					C4-C5	1.4571(3)
C5-C6	1.4746(1)					C5-C6	1.3701(3)
C6-C1	1.3607(1)					C6-C1	1.4552(4)
C1-O1	1.2336(1)	C7-O3	1.2517(1)	C1-O1	1.2125(8)	C1-O1	1.2483(3)
C4-O2	1.2320(1)					C4-O2	1.2510(3)
C2-Cl1	1.7143(1)	C8-Cl5	1.7174(1)	C2-Cl1	1.6984(5)	C2-Cl1	1.7222(3)
C3-Cl2	1.7145(1)	C9-Cl6	1.7219(1)	C3-Cl2	1.7000(5)	C3-Cl2	1.7243(2)
C5-Cl3	1.7125(1)					C5-Cl3	1.7215(3)
C6-Cl4	1.7147(1)					C6-Cl4	1.7230(3)
τ / °	3.8		2.7		0.0		3.6

Table S5. Topology of electron density in chemical bonds. Computed from XRD based densities.

Bond	Length (Å)	Electron Density (eÅ^{-3}) ρ_{cp}	Laplacian (eÅ^{-3})	Ellipticity	Bond order n_{topo}
C1-O1	1.2339(3)	2.778	-26.4	0.03	1.41
C4-O2	1.2323(3)	2.920	-33.8	0.10	1.60
C1-C2	1.4760(4)	1.870	-13.3	0.23	0.97
C2-C3	1.3622(3)	2.231	-21.3	0.35	1.57
C3-C4	1.4738(4)	1.866	-13.4	0.25	0.94
C4-C5	1.4752(3)	1.883	-13.8	0.15	0.96
C5-C6	1.3604(3)	2.236	-20.9	0.31	1.53
C6-C1	1.4746(4)	1.802	-12.1	0.23	0.87
C2-Cl1	1.7145(3)	1.422	-3.6	0.07	
C3-Cl2	1.7146(2)	1.428	-4.0	0.06	
C5-Cl3	1.7127(3)	1.344	-1.5	0.18	
C6-Cl4	1.7151(3)	1.486	-4.0	0.07	
C7-O3	1.2524(1)	2.676	-26.7	0.03	1.45
C7-C8	1.5441(1)	1.941	-14.1	0.16	1.05
C7-C9*	1.3725(1)	2.165	-19.4	0.30	1.06
C8-C9	1.4545(1)	1.932	-14.5	0.22	1.45
C8-Cl5	1.7175(1)	1.384	-2.5	0.19	
C9-Cl6	1.7221(1)	1.405	-3.2	0.07	
C10-N1	1.3526(1)	2.157	-22.5	0.10	1.20
C14-N1	1.3581(1)	2.161	-22.5	0.11	1.20
N1-C15	1.4689(1)	1.696	-10.7	0.05	1.02
C12-N2	1.3417(1)	2.431	-21.5	0.32	1.42
N2-C16	1.4626(1)	1.687	-7.8	0.09	1.05
N2-C17	1.4633(1)	1.697	-8.5	0.09	1.05
C10-C11	1.3692(1)	2.149	-18.5	0.25	1.40
C11-C12	1.4226(1)	2.002	-16.0	0.17	1.16
C12-C13	1.4250(1)	1.983	-16.0	0.17	1.14
C13-C14	1.3681(1)	2.153	-18.6	0.24	1.42
C10-H10	1.0830	1.746	-19.6	0.06	0.85
C11-H11	1.0830	1.737	-16.8	0.06	0.92
C13-H13	1.0830	1.719	-16.6	0.06	0.91
C14-H14	1.0830	1.748	-19.4	0.06	0.85
C15-H15A	1.0770	1.668	-15.9	0.10	0.94
C15-H15B	1.0770	1.626	-17.3	0.11	1.01

C15-H15C	1.0770	1.649	-15.4	0.10	0.94
C16-H16A	1.0770	1.525	-9.9	0.21	0.96
C16-H16B	1.0770	1.681	-13.6	0.21	1.03
C16-H16C	1.0770	1.625	-12.8	0.20	0.99
C17-H17A	1.0770	1.651	-15.9	0.10	0.91
C17-H17B	1.0770	1.690	-14.3	0.11	1.00
C17-H17C	1.0770	1.672	-16.0	0.10	0.93

Table S6 Intermolecular critical points in the title compound. Computed from XRD based densities.

A…B	Rho tot	Laplacian	type	Symm. operation on *A*
Trimer				
Cl1⋯Cl5	0.0322	0.41	(3,-1)	1–*x*, 1–*y*, 1–*z*
Cl1⋯Cl6	0.0575	0.72	(3,-1)	1–*x*, 1–*y*, 1–*z*
Cl2⋯Cl6	0.0455	0.57	(3,-1)	1–*x*, 1–*y*, 1–*z*
O1⋯C7	0.0473	0.61	(3,-1)	1–*x*, 1–*y*, 1–*z*
C2⋯C9	0.0771	0.81	(3,-1)	1–*x*, 1–*y*, 1–*z*
C8⋯Cl1	0.0317	0.40	(3,+1)	1–*x*, 1–*y*, 1–*z*
C9⋯Cl1	0.0539	0.67	(3,+1)	1–*x*, 1–*y*, 1–*z*
C9⋯Cl2	0.0428	0.55	(3,+1)	1–*x*, 1–*y*, 1–*z*
O1⋯C8	0.0427	0.55	(3,+1)	1–*x*, 1–*y*, 1–*z*
C4⋯C9	0.0647	0.78	(3,+1)	1–*x*, 1–*y*, 1–*z*
C6⋯C7	0.455	0.56	(3,+1)	1–*x*, 1–*y*, 1–*z*
C6⋯C9	0.0695	0.76	(3,+1)	1–*x*, 1–*y*, 1–*z*
Inter-trimers				
Cl1⋯Cl3	0.0425	0.54	(3,-1)	1–*x*, 2–*y*, 1–*z*
Cl2⋯Cl4	0.0383	0.51	(3,-1)	1–*x*, 2–*y*, 1–*z*
Cl4⋯C3	0.0391	0.47	(3,-1)	1–*x*, 2–*y*, 1–*z*
C1⋯C5	0.0257	0.28	(3,-1)	1–*x*, 2–*y*, 1–*z*
C5⋯C3	0.0226	0.26	(3,+1)	1–*x*, 2–*y*, 1–*z*
Cl1⋯C5	0.0245	0.29	(3,+1)	1–*x*, 2–*y*, 1–*z*
Cl3⋯C1	0.0245	0.29	(3,+1)	1–*x*, 2–*y*, 1–*z*
Cl4⋯C4	0.0194	0.22	(3,+1)	1–*x*, 2–*y*, 1–*z*
C2⋯C6	0.0226	0.26	(3,+1)	1–*x*, 2–*y*, 1–*z*
C3⋯C1	0.0194	0.22	(3,+1)	1–*x*, 2–*y*, 1–*z*
C3⋯C6	0.0186	0.21	(3,+1)	1–*x*, 2–*y*, 1–*z*
Other contacts				
Cl4⋯C16	0.0256	0.34	(3,-1)	1–*x*, 1–*y*, 1–*z*
H16A⋯O1	0.0455	0.61	(3,-1)	1–*x*, 1–*y*, 1–*z*
H11⋯Cl6	0.0589	0.66	(3,-1)	1–*x*, 1–*y*, 1–*z*

Table S7 Geometric parameters of hydrogen bonds.

	D–H / Å	H···*A* / Å	*D*···*A* / Å	*D*–H···*A* / °	Symm. op. on *A*
C10–H10···O3	1.08	2.21	2.9744(1)	126	*x*, *y*, *z*
C11–H11···Cl6	1.08	2.81	3.5363(1)	124	1–*x*, 1–*y*, 1–*z*
C13–H13···Cl5	1.08	2.72	3.7663(5)	162	–*x*, –*y*, –*z*
C14–H14···O1	1.08	2.32	3.1908(1)	136	–1+*x*, –1+*y*, –1+*z*
C15–H15A···O2	1.08	2.33	3.3464(1)	157	–*x*, 1–*y*, –*z*
C15–H15C···O2	1.08	2.39	3.4665(1)	174	*x*, *y*, *z*
C16–H16B···O2	1.08	2.57	3.3428(1)	128	*x*, –1+*y*, *z*
C17–H17B···O3	1.08	2.29	3.3615(1)	176	–*x*, –*y*, –*z*
C17–H17C···Cl5	1.08	2.79	3.8109(1)	157	*x*, –1+*y*, –1+*z*

Orbital analogy between the σ-allyl cation and π-stacked trimers of tetrachloroquinone anions

The analogy with the σ-allyl radical and the σ-allyl cation are illustrated in Figure S12. Here the local π-orbital bearing atom may be a carbon or silicon that overlap with their neighbour(s) via σ-bonding. The major difference with respect to the presented trimer is the absence of the $–(CH_2)_3–$ alkyl linked cages which provide through bond stabilization for the symmetrical σ-allyl radical and σ-allyl cation. The insight of Olson was that by using silicon as the provider of the (two in the case of the cation and three in the case of the radical) electrons delocalized bonding interaction occurs in the lowest σ-allyl orbital illustrated in Figure S12c providing the driving force for equal bond distances among the Si atoms maintaining a D_{3h} symmetry. In the case of carbons the symmetry is lowered to C_{3v}. Presumably due to the smaller atomic size localized electron pair bonding is preferred in the cases with carbon atoms providing the local π-orbitals and π -electrons. By analogy to the quinone trimer, both our experiments and computations indicate that the symmetrical arrangement is preferred.

a

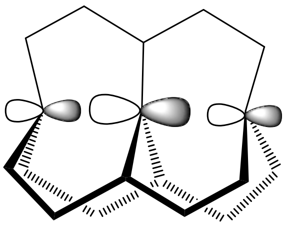

b

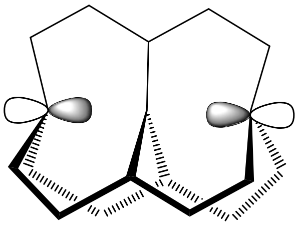

c

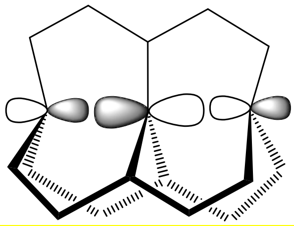

Figure S12. Local π-orbitals are the basis to provide three delocalized orbitals in the model of a σ-allyl radical (three π-electrons) and a σ-allyl cation (two π-electrons). In the quinone trimer dianions the overlap is similar but the role of the single atomic orbitals are played by the delocalized LUMO orbitals of the quinone.

Cartesian coordinates of the converged geometries and the corresponding absolute energies (in Hartrees).

Table S8 Cartesian coordinates of the converged geometries and the corresponding absolute energies (in Hartrees).

Min-1: UM05-2X/6-311G (d,p), -6659.87319650 a.u.

17	2.687002000	3.483987000	1.592721000
17	2.687037000	3.483053000	-1.593218000
17	-2.687037000	3.483053000	-1.593218000
17	-2.687002000	3.483987000	1.592721000
8	0.000000000	3.263400000	2.688485000
8	0.000000000	3.263248000	-2.688911000
6	0.000000000	3.241674000	1.474060000
6	1.241927000	3.291146000	0.675903000
6	1.241939000	3.290848000	-0.676341000
6	0.000000000	3.241390000	-1.474487000

6	-1.241939000	3.290848000	-0.676341000
6	-1.241927000	3.291146000	0.675903000
17	2.696343000	0.000000000	1.590931000
17	2.696373000	0.000000000	-1.589979000
17	-2.696373000	0.000000000	-1.589979000
17	-2.696343000	0.000000000	1.590931000
8	0.000000000	0.000000000	2.705991000
8	0.000000000	0.000000000	-2.705073000
6	0.000000000	0.000000000	1.486405000
6	1.231323000	0.000000000	0.679988000
6	1.231324000	0.000000000	-0.679061000
6	0.000000000	0.000000000	-1.485491000
6	-1.231324000	0.000000000	-0.679061000
6	-1.231323000	0.000000000	0.679988000
17	2.687002000	-3.483987000	1.592721000
17	2.687037000	-3.483053000	-1.593218000
17	-2.687037000	-3.483053000	-1.593218000
17	-2.687002000	-3.483987000	1.592721000
8	0.000000000	-3.263400000	2.688485000
8	0.000000000	-3.263248000	-2.688911000
6	0.000000000	-3.241674000	1.474060000
6	1.241927000	-3.291146000	0.675903000
6	1.241939000	-3.290848000	-0.676341000
6	0.000000000	-3.241390000	-1.474487000
6	-1.241939000	-3.290848000	-0.676341000
6	-1.241927000	-3.291146000	0.675903000

Min-2A. UM05-2X/6-311G (d,p), -6659.89681878 a.u.

17	1.756073000	3.636536000	-0.921053000
17	0.016247000	3.995764000	-3.581760000
17	-4.452688000	2.884963000	-0.793218000
17	-2.698856000	2.531864000	1.859814000
8	0.155516000	2.636940000	1.295894000
8	-2.797466000	3.445298000	-3.113608000
6	-0.513650000	2.830784000	0.301011000
6	0.077108000	3.261948000	-0.985818000
6	-0.662490000	3.430696000	-2.100574000
6	-2.127684000	3.229100000	-2.126394000
6	-2.728495000	2.917941000	-0.811018000
6	-1.991601000	2.748951000	0.305551000
17	-3.107204000	-0.350026000	0.074298000
17	-1.354323000	-0.756633000	2.715798000
8	-1.510313000	0.658350000	-2.153334000
6	-0.820599000	0.316193000	-1.186583000
6	-1.394236000	-0.114585000	0.083440000
6	-0.636282000	-0.389047000	1.186578000
17	3.107204000	0.350026000	-0.074298000
17	1.354323000	0.756633000	-2.715798000
8	1.510313000	-0.658350000	2.153334000
6	0.820599000	-0.316193000	1.186583000
6	1.394236000	0.114585000	-0.083440000
6	0.636282000	0.389047000	-1.186578000
17	-1.756073000	-3.636536000	0.921053000
17	-0.016247000	-3.995764000	3.581760000
17	4.452688000	-2.884963000	0.793218000
17	2.698856000	-2.531864000	-1.859814000
8	-0.155516000	-2.636940000	-1.295894000
8	2.797466000	-3.445298000	3.113608000
6	0.513650000	-2.830784000	-0.301011000
6	-0.077108000	-3.261948000	0.985818000
6	0.662490000	-3.430696000	2.100574000
6	2.127684000	-3.229100000	2.126394000
6	2.728495000	-2.917941000	0.811018000
6	1.991601000	-2.748951000	-0.305551000

Min-2B. UM05-2X/6-311G (d,p), -6659.90684782 a.u.

17	1.710055000	3.668366000	-1.004510000
17	-0.039257000	4.195536000	-3.613444000
17	-4.512777000	3.098285000	-0.814135000
17	-2.746823000	2.573319000	1.783236000
8	0.114481000	2.651618000	1.215883000
8	-2.890193000	3.791633000	-3.138577000
6	-0.573602000	2.961419000	0.238085000
6	-0.000027000	3.413119000	-1.024011000
6	-0.753442000	3.664479000	-2.129844000
6	-2.207623000	3.541593000	-2.145793000
6	-2.784484000	3.165914000	-0.858956000
6	-2.030861000	2.914032000	0.246650000
17	-3.109853000	-0.447242000	0.046457000
17	-1.369405000	-0.654370000	2.751733000
8	-1.454332000	0.311208000	-2.204978000
6	-0.792989000	0.134842000	-1.216197000

6	-1.414084000	-0.209182000	0.095718000
6	-0.688688000	-0.307316000	1.218401000
17	3.109853000	0.447242000	-0.046457000
17	1.369405000	0.654370000	-2.751733000
8	1.454332000	-0.311208000	2.204978000
6	0.792989000	-0.134842000	1.216197000
6	1.414084000	0.209182000	-0.095718000
6	0.688688000	0.307316000	-1.218401000
17	-1.710055000	-3.668366000	1.004510000
17	0.039257000	-4.195536000	3.613444000
17	4.512777000	-3.098285000	0.814135000
17	2.746823000	-2.573319000	-1.783236000
8	-0.114481000	-2.651618000	-1.215883000
8	2.890193000	-3.791633000	3.138577000
6	0.573602000	-2.961419000	-0.238085000
6	0.000027000	-3.413119000	1.024011000
6	0.753442000	-3.664479000	2.129844000
6	2.207623000	-3.541593000	2.145793000
6	2.784484000	-3.165914000	0.858956000
6	2.030861000	-2.914032000	-0.246650000

Min-3. (Face-to-edge) UM05-2X/6-311G (d,p), -6659.90522498 a.u.

17	2.685402000	-1.976175000	3.201050000
17	2.696900000	-3.810013000	5.813484000
17	-2.696900000	-3.810013000	5.813484000
17	-2.685402000	-1.976175000	3.201050000
8	0.000000000	-1.331550000	2.305499000
8	0.000000000	-4.448269000	6.736873000
6	0.000000000	-2.044980000	3.318287000
6	1.221423000	-2.499746000	3.958531000
6	1.219703000	-3.284046000	5.073476000
6	0.000000000	-3.739419000	5.725228000
6	-1.219703000	-3.284046000	5.073476000
6	-1.221423000	-2.499746000	3.958531000
17	2.704385000	-1.255693000	-0.993492000
17	2.704385000	1.255693000	0.993492000
17	-2.704385000	1.255693000	0.993492000
17	-2.704385000	-1.255693000	-0.993492000
8	0.000000000	-2.101581000	-1.609616000
8	0.000000000	2.101581000	1.609616000
6	0.000000000	-1.139089000	-0.892496000
6	1.271145000	-0.520346000	-0.414455000
6	1.271145000	0.520346000	0.414455000
6	0.000000000	1.139089000	0.892496000
6	-1.271145000	0.520346000	0.414455000
6	-1.271145000	-0.520346000	-0.414455000
17	2.696900000	3.810013000	-5.813484000
17	2.685402000	1.976175000	-3.201050000
17	-2.685402000	1.976175000	-3.201050000
17	-2.696900000	3.810013000	-5.813484000
8	0.000000000	4.448269000	-6.736873000
8	0.000000000	1.331550000	-2.305499000
6	0.000000000	3.739419000	-5.725228000
6	1.219703000	3.284046000	-5.073476000
6	1.221423000	2.499746000	-3.958531000
6	0.000000000	2.044980000	-3.318287000
6	-1.221423000	2.499746000	-3.958531000
6	-1.219703000	3.284046000	-5.073476000

References

[1] K. Molčanov, V. Stilinović, A. Šantić, N. Maltar-Strmečki, D. Pajić, B. Kojić-Prodić, *Cryst. Growth Des.* **2016**, *16*, 4777-4782.

[2] http://ewww.mpi-muelheim.mpg.de/bac/logins/bill/julX en.php

[3] CrysAlis^{Pro}, *Rigaku Oxford Diffraction*, **2017**, version: 1.171.39.13a, Rigaku Corporation, Oxford, UK.

[4] O.V. Dolomanov, L. J. Bourhis, R. J. Gildea, J. A. K. Howard, H. Puschmann, *J. Appl. Cryst*. **2009**, *42*, 339-341.

[5] G. M. Sheldrick, *Acta Cryst. A* **2015**, *A71*, 3-8.

[6] C. Jelsch, B. Guillot, A. Lagoutte, C. Lecomte, *J. Appl. Crystallogr.* **2005**, *38*, 38-54.

[7] A. Ø. Madsen, *J Appl. Cryst*. **2006**, *39*, 757-758.

[8] B. Guillot, *Acta Crystallogr. A* **2012**, *68*, s204; B. Guillot, F. Enrique, K. Huder, C. Jelsch, *Acta Cryst. A* **2014**, *70*, C279.

[9] L. J. Farrugia, *J. Appl. Crystallogr.* **1997**, *30*, 565.

[10] B. Zarychta, Z. Zaleski, J. Kyzioł, Z. Dazskiewicz, C. Jelsch, *Acta Cryst. B* **2011**, *B67*, 250-262.

[11] S. T. Howard, O. Lamarche, *J. Phys. Org. Chem.* **2003**, *16*, 133-141.

[12] V. G. Tsirelson, E. V. Bartashevich, A. I. Stash, V. A. Potemkin, *Acta Crystallogr. B* **2007**, *B63*, 142-150.

[13] E. A. Zhurova, V. V. Zhurov, A. A. Pinkerton, *J. Am. Chem. Soc.* **2007**, *129*, 13887-13893.
[14] K. Molčanov, C. Jelsch, E. Wenger, V. Stilinović, B. Kojić-Prodić, B. Landeros, E. C. Escudero, submitted to *J. Am. Chem. Soc*.
[15] D. Cremer, J. A. Pople, *J. Amer. Chem.Soc.* **1975**, *97*, 1354-1358.
[16] *Gaussian 16, Revision A.03*, M. J. Frisch, G. W. Trucks, H. B. Schlegel, G. E. Scuseria, M. A. Robb, J. R. Cheeseman, G. Scalmani, V. Barone, G. A. Petersson, H. Nakatsuji, X. Li, M. Caricato, A. V. Marenich, J. Bloino, B. G. Janesko, R. Gomperts, B. Mennucci, H. P. Hratchian, J. V. Ortiz, A. F. Izmaylov, J. L. Sonnenberg, D. Williams-Young, F. Ding, F. Lipparini, F. Egidi, J. Goings, B. Peng, A. Petrone, T. Henderson, D. Ranasinghe, V. G. Zakrzewski, J. Gao, N. Rega, G. Zheng, W. Liang, M. Hada, M. Ehara, K. Toyota, R. Fukuda, J. Hasegawa, M. Ishida, T. Nakajima, Y. Honda, O. Kitao, H. Nakai, T. Vreven, K. Throssell, J. A. Montgomery, Jr., J. E. Peralta, F. Ogliaro, M. J. Bearpark, J. J. Heyd, E. N. Brothers, K. N. Kudin, V. N. Staroverov, T. A. Keith, R. Kobayashi, J. Normand, K. Raghavachari, A. P. Rendell, J. C. Burant, S. S. Iyengar, J. Tomasi, M. Cossi, J. M. Millam, M. Klene, C. Adamo, R. Cammi, J. W. Ochterski, R. L. Martin, K. Morokuma, O. Farkas, J. B. Foresman, D. J. Fox, Gaussian, Inc., Wallingford CT, **2016**.
[17] K. B. Lipkowitz, R. M. Larter, D. B. Boyd, *J. Am. Chem. Soc*. **1981**, 102, 85.
[18] K.K. Baldridge, J. Leahy, J. S. Siegel, *Tetrahedron Lett*. **1999**, 40, 3503.
[19] L. P. Olson, *Org. Lett.* **2000**, *2*, 3059.